Stopped-Flow, Classical, and Dynamic Light Scattering Analysis of Matrix Protein Binding to Nucleocapsids of Vesicular Stomatitis Virus†

Douglas S. Lyles,*,‡ Margie O. McKenzie,‡ and Roy R. Hantgan§

Department of Microbiology and Immunology and Department of Biochemistry, Bowman Gray School of Medicine of Wake Forest University, Winston-Salem, North Carolina 27157-1064

Received August 22, 1995; Revised Manuscript Received February 6, 1996⊗

ABSTRACT: During the process of assembly of enveloped viruses, binding of the nucleoprotein core of the virus (nucleocapsid) to the host membrane is mediated by the viral matrix (M) protein. Light scattering properties of vesicular stomatitis virus (VSV) nucleocapsids and nucleocapsid-M protein (NCM) complexes assembled *in vivo* were determined following solubilization of the virion envelope with detergents at varying ionic strength to vary the extent of M protein binding. Three factors were found to contribute to the light scattering properties of VSV nucleocapsids: their conformation, extent of self-association, and amount of bound M protein. All three were affected by changes in ionic strength but could be distinguished by several parameters. Conformational changes in nucleocapsids and NCM complexes occurred rapidly (millisecond time scale) upon changing salt concentration and were reflected in changes in the angular dependence of light scattering intensity (i.e., changes in radius of gyration, R_G). Changes in extent of self-association occurred relatively slowly (seconds to minutes time scale) and could be distinguished by the concentration dependence of the apparent molecular mass and diffusion coefficient of the NCM complex. Changes in M protein binding occurred on an intermediate time scale ($t_{1/2}$ approximately 1 s) and reflected changes in both molecular mass and R_G. The data presented here provide criteria for assessing binding of M protein to nucleocapsids under conditions of minimal perturbation of the NCM complex assembled *in vivo* and at low protein concentrations so that self-association of the NCM complex was minimal and reversible.

During the process of assembly of enveloped viruses by budding from host membranes, the nucleoprotein core of the virus (nucleocapsid) binds to the cytoplasmic surface of the host membrane. For most enveloped viruses, binding of the nucleocapsid to the host membrane is mediated by the viral matrix (M) protein. Vesicular stomatitis virus (VSV) is the prototype rhabdovirus, which has been widely used in studies of virus assembly. The nucleocapsid of VSV is a helical structure containing the 11 kb single-strand RNA genome encapsidated by 1300 copies of a single major nucleoprotein (N protein) and lesser amounts of two polymerase-associated proteins, P and L (Thomas et al., 1985). The virion contains approximately 2000 copies of M protein, which remain bound to the nucleocapsid when the envelope is solubilized with detergents in low ionic strength buffers. The resulting nucleocapsid-M protein (NCM) complex is a tightly coiled helical structure that has the same morphology as the internal contents of the virion and appears to give the virion its characteristic bullet-like shape (Barge et al., 1993; Newcomb & Brown, 1981; Newcomb et al., 1982).

VSV nucleocapsids largely devoid of M protein can be isolated by solubilizing the virion envelope with detergents in high ionic strength buffers (e.g., 0.25 M NaCl). In contrast to the tightly coiled, bullet-shaped NCM complex, nucleocapsids lacking M protein are loosely coiled and flexible (Newcomb & Brown, 1981). NCM complexes containing intermediate amounts of M protein can be isolated at intermediate salt concentrations (Kaptur et al., 1991) and probably contain a mixture of coiled and uncoiled regions (Newcomb et al., 1982; Odenwald et al., 1986). When the VSV M protein is dissociated from the nucleocapsid in high ionic strength, it is capable of reassociating with the nucleocapsid upon removal of the salt by dialysis, resulting in an NCM complex with the same morphology as the original NCM complex (Newcomb et al., 1982). For many enveloped viruses, solubilization of the envelope at low salt concentrations results in association of their matrix proteins with the nucleocapsid. However, VSV is perhaps the only virus in which the resulting structure has the same distinctive morphology seen in virions. It is also the only virus in which the reversible dissociation and reassociation of M protein with the nucleocapsid has been shown to result in the same morphology.

Despite the important role of M protein binding to nucleocapsids in virus assembly, relatively few investigators have examined this process using *in vitro* biochemical methods. This reluctance stems in large part from two concerns. First, in the absence of criteria for their native activity, there is little assurance that binding of isolated M proteins to nucleocapsids *in vitro* involves the same interac-

† This work was supported by Public Health Service Grant AI15892 from the National Institute of Allergy and Infectious Diseases. The stopped-flow facility and the argon-ion laser used in the dynamic light scattering experiments were supported by grants from the North Carolina Biotechnology Center.

* To whom correspondence should be addressed.

‡ Department of Microbiology and Immunology.

§ Department of Biochemistry.

⊗ Abstract published in *Advance ACS Abstracts,* May 1, 1996.

[1] Abbreviations: G, envelope glycoprotein; L, large RNA polymerase subunit; M, matrix protein; N, nucleocapsid protein; NCM, nucleocapsid-M protein (complex); P, phosphoprotein polymerase subunit; R_G, radius of gyration; R_S, Stokes radius; SDS−PAGE, sodium dodecyl sulfate−polyacrylamide gel electrophoresis; VSV, vesicular stomatitis virus.

S0006-2960(95)02001-0 CCC: $12.00 © 1996 American Chemical Society

tions as binding *in vivo*. Second, the M proteins of most viruses have a tendency to self-associate when isolated *in vitro*, especially at low or intermediate ionic strength. Some aggregated viral M proteins resemble intermediates in virus assembly in infected cells when viewed by electron microscopy, suggesting that self-association of M proteins may play a role in virus assembly (Gaudin et al., 1995; Heggeness et al., 1982a). However, M proteins usually enter the virus assembly pathway as soluble proteins in the cytoplasm (e.g., Atkinson et al., 1976; Knipe et al., 1977; McCreedy et al., 1990), so that aggregated forms of M protein are suspect.

In order to develop criteria for the activity of native M protein, we have used light scattering analysis to determine the biochemical behavior of the VSV M protein and nucleocapsid following solubilization of the virion envelope with detergents. These experiments address the above concerns about *in vitro* binding studies with M protein as follows: First, the M protein bound to the nucleocapsid following solubilization of the envelope was bound to the nucleocapsid *in vivo* and represents the native interaction as shown by the distinctive morphology of the VSV NCM complex (Newcomb & Brown, 1981). The properties of the nucleocapsid (or NCM complex) can be evaluated without further isolation, since it is very large compared to the envelope components solubilized in detergent micelles. Thus the analysis can be performed either immediately after solubilization of the envelope or else after further purification of the components. Second, since light scattering analysis is very sensitive to the mass of the particle, the extent of self-association of M protein or nucleocapsids can be evaluated and conditions can be sought which minimize its effects. Finally, light scattering analysis is well-suited to studying large particles such as nucleocapsids. Relatively low protein concentrations can be used. Information about the conformation of the nucleocapsid can be obtained from the angular dependence of light scattering intensity. Also, information can be gained about binding mechanisms, since light scattering data can be analyzed kinetically as well as under equilibrium conditions.

Light scattering properties of VSV nucleocapsids and NCM complexes assembled *in vivo* were determined following solubilization of the virion envelope with detergents at varying ionic strength to vary the extent of M protein binding. Light scattering of NCM complexes was found to be affected by three factors: M protein binding, conformational changes, and self-association. These factors could be distinguished by their effects on intensity and angular dependence of light scattering, diffusion coefficients measured by dynamic light scattering analysis, and kinetics of light scattering changes determined by stopped-flow analysis. These studies establish criteria for the behavior of nucleocapsids and NCM complexes by which future *in vitro* binding studies can be evaluated.

EXPERIMENTAL PROCEDURES

Purification of Virions and Nucleocapsids. Radiolabeled VSV (San Juan strain, Indiana serotype) was prepared by growth in BHK cells in the presence of [^{35}S]methionine, purified by sucrose gradient centrifugation, and assayed for protein concentration and specific radioactivity as described (Kaptur et al., 1991). The purified virus was dialyzed overnight against 10 mM Tris, pH 7.8, at 4 °C and used immediately without freezing and thawing.

Nucleocapsids were purified as described by Newcomb et al. (1982) with minor modifications. Briefly, virion envelopes were solubilized in 10 mM Tris, 0.25 M NaCl, 1% Triton X-100, pH 8.1, and nucleocapsids were isolated by centrifugation on a 10−70% sucrose gradient for 90 min at 38 000 rpm in a Beckman SW41 rotor. The gradient was collected into 1 mL fractions, and the radioactivity of each fraction was determined by scintillation counting. The fractions containing nucleocapsids were pooled and dialyzed overnight at 4 °C against 10 mM Tris, pH 7.8.

Light Scattering Intensity Measurements. Buffers used for light scattering measurements were filtered through a 0.2 μm filter before use to remove dust particles and aggregates of Triton X-100. Virions were centrifuged at 600*g* for 10 min to remove virus aggregates. Samples for light scattering measurements of NCM complexes were prepared by diluting virions into 10 mM Tris, 10 mM NaCl, and 0.1% Triton X-100, pH 8.1, and then filtering the sample through a 0.8 μm filter into a dust-free 1 cm diameter cylindrical cuvette. Recovery of viral protein following filtration was routinely >90%. Light scattering intensity measurements were made as a function of detector angle (Θ) at 25.0 ± 0.1 °C using a motor-driven, computer-controlled goniometer and photon counting detector (Brookhaven Instruments BI-200SM) and vertically polarized light (633 nm) from a 35 mW Spectra-Physics 127 He−Ne laser as described (Hantgan et al., 1993). Following the initial measurements on intact NCM complexes, 5 M NaCl was added to adjust the NaCl to the desired concentration to dissociate M protein. The sample was allowed to equilibrate for 10 min, and the light scattering measurements were repeated. Similar results were obtained by diluting virions directly into buffer containing the desired NaCl concentration. Light scattering measurements on a benzene standard and a buffer blank lacking viral proteins were made under identical conditions. Following the light scattering measurements, an aliquot of the sample was taken for liquid scintillation counting, the sample was centrifuged at 100000*g* for 45 min to pellet the nucleocapsids or NCM complexes, and radioactivity of an aliquot of the supernatant was determined. The protein concentration due to nucleocapsids or NCM complexes was calculated by subtracting the radioactivity of the supernatant from the total radioactivity.

Analysis of Light Scattering Intensity Data. The angular dependence data were analyzed according to Rayleigh theory to obtain the weight average molecular mass and shape function for nucleocapsids and NCM complexes (Marshall, 1978). The Rayleigh ratio of the sample $R(\Theta)$ was calculated as follows:

$$R(\Theta) = \frac{\text{IST(sample)} - \text{IST(blank)}}{\text{IST(standard)}} R(\text{standard}) \quad (1)$$

where IST is the raw photon count data (I) corrected for sample geometry ($I \sin \Theta$) and R(standard) = 9.39×10^{-6} cm^{-1}, the Rayleigh ratio of the benzene standard for vertically polarized light at 633 nm (Pike et al., 1975) corrected for the refractive index difference between benzene and water (Carr et al., 1977). $R(\Theta)$ was used to determine the apparent molecular mass, M_{app}, and shape function, $P(\Theta)$:

$$\frac{R(\Theta)}{Kc} = M_{app} P(\Theta) \quad (2)$$

where $K = [4\pi^2 n_0^2 (dn/dc)^2]/\lambda_0^4 N_0$, c is the protein concentration of nucleocapsids or NCM complexes (in g/cm^3), n_0 is the refractive index of the solvent, $\lambda_0 = 633$ nm, N_0 is Avogadro's number, and dn/dc is the refractive index increment for a typical protein in the presence of Triton X-100, estimated to be 0.243 cm^3/g at 633 nm (Rivas et al., 1991). M_{app} is related to the true molecular mass, M, by $(1/M_{app}) = (1/M) + 2A_2c$, where A_2 is the molecular interaction constant (second virial coefficient). To account for potential intermolecular interactions, each measurement was repeated at a series of protein concentrations. In cases where M_{app} was not independent of concentration, the data were extrapolated to $c = 0$.

The values of $R(\Theta)/Kc$ for nucleocapsids were fit to eq 2 using a nonlinear least-squares fit (JMP statistical analysis software, SAS Institute, Inc., Cary, NC) of two parameters, M and R_G, and the shape function for a random coil (Marshall, 1978):

$$P(\Theta) = \frac{2}{a^2}[\exp(-a) + a - 1] \qquad (3)$$

where $a = (16\pi^2/\lambda^2)R_G^2 \sin^2(\Theta/2)$ and R_G is the radius of gyration.

In the case of NCM complexes, the shape function is not well-defined. However, it was observed that a plot of $Kc/R(\Theta)$ versus $\sin^2(\Theta/2)$ approximated a straight line (see Results). Therefore, the data were analyzed by linear least-squares fit to the classical light scattering equation:

$$\frac{Kc}{R(\Theta)} = \frac{1}{M}\left[1 + \frac{16\pi^2 n_0^2 R_G^2}{3\lambda_0^2}\sin^2(\Theta/2)\right] \qquad (4)$$

Equation 4 is valid only at small angles or for cases where the light scattering particle is much smaller than the wavelength of the scattered light, which was clearly not the case for these data. However, the linearity of the plot of $Kc/R(\Theta)$ versus $\sin^2(\Theta/2)$ allowed an apparent molecular mass to be calculated from the y-intercept and an apparent R_G to be determined from the ratio of the slope to the y-intercept.

Dynamic Light Scattering Analysis. The translational diffusion of nucleocapsids and NCM complexes was measured by dynamic light scattering analysis using the same apparatus and sample preparation procedures as the light scattering intensity measurements. The light source was vertically polarized light (488 nm) from an INNOVA 307 argon ion laser (Coherent). The detector output was analyzed with a Brookhaven Instruments BI-2030AT correlator as described (Hantgan et al., 1993) at angles from 45° to 130°. For all of the samples analyzed, the light scattering intensity of the buffer blank was ≤5% of the sample intensity so that diffusion of Triton X-100 micelles made a negligible contribution to the diffusion measurement. The intensity-normalized autocorrelation functions [$C'(t)$] at each angle were calculated by dividing the value in each correlator channel [$C(t)$] by the baseline (uncorrelated) value determined from the average of 6 correlator channels with long delay times. The values of $C(t)$ were fit to an exponential decay using second-order cumulants analysis (Koppel, 1972) using software supplied by the manufacturer, which gives an average rate constant, Γ, and a second moment to account for the distribution of particle sizes. Since $\Gamma = D_t(4\pi n_0/\lambda_0)^2 \sin^2(\Theta/2)$, the translational diffusion coefficient, D_t, was calculated from the slope of a plot of Γ versus $\sin^2(\Theta/2)$. The Stokes radius R_S was calculated from $D_t = kT/6\pi\eta R_S$, where η is the solvent viscosity.

Stopped-Flow Analysis. Time courses for the changes in light scattering intensity of NCM complexes upon shifting the concentration of NaCl were determined using an Applied Photophysics DX.17MV stopped-flow spectrophotometer at a wavelength of 500 nm and the detector at a 90° angle to the light path. NCM complexes in buffer containing 10 mM NaCl and 0.1% Triton X-100 were prepared as described above and placed in the sample syringe. The second syringe contained the same buffer with twice the desired final NaCl concentration. Equal volumes from each syringe were injected into the mixing chamber, and 400 data points were collected using a split time base in which 200 data points were collected from either 0 to 2 s or 0 to 5 s to determine the fast phase, and 200 data points were collected in the subsequent 100 s to determine the slower phase. A total of four reaction traces were collected at each NaCl concentration. The data from 0.4 to 105 s were fit either to a single exponential, $I(t) = I_1 e^{-k_1 t} + I_f$, or to a double exponential, $I(t) = I_1 e^{-k_1 t} + I_2 e^{-k_2 t} + I_f$, by a nonlinear least squares fit of 3 parameters (I_1, k_1, I_f) or five parameters (I_1, k_1, I_2, k_2, I_f), respectively, using software supplied by the manufacturer. A single exponential was assumed to fit the data unless the normalized variance was reduced by at least a factor of 2 by assuming a double exponential. In most cases where a double exponential was found, the improvement in the fit reduced the variance by a factor of 5−10. The salt-dependent conformational changes in nucleocapsids were determined similarly except that the time base was 100 ms.

RESULTS

Intensity and Angular Dependence of Light Scattering by VSV Nucleocapsids. Before investigating the binding of VSV M protein to nucleocapsids, it was necessary to determine the light scattering properties of nucleocapsids lacking M protein. Consideration of the composition of VSV and the products that result from solubilization of the envelope with detergents in high ionic strength buffers (Table 1) suggests that light scattering by the viral nucleocapsid should be several orders of magnitude greater than that of the solubilized envelope components. Light scattering intensity at any given detector angle is proportional to the molecular mass and concentration of the light scattering species. The mass of the nucleocapsid is approximately 90 MDa (Thomas et al., 1985) and its concentration is 46% of the total protein concentration. In contrast, the transmembrane envelope glycoprotein (G protein) is an approximately 0.2 MDa trimer of identical 0.062 MDa subunits (Doms et al., 1987; Lyles et al., 1990) and is 24% of the total protein concentration, while soluble M protein is a monomer [0.026 MDa (McCreedy et al., 1990)] and is 30% of the total protein. The viral lipids (average mass 750 Da) make a negligible contribution to the mass and concentration of detergent micelles (usually 0.1% Triton X-100), which are included in the buffer blank that would be subtracted from every light scattering measurement. The data in Figure 1 confirm this analysis.

The envelopes of VSV virions (16.5 μg/mL total protein) were solubilized with Triton X-100 in the presence of 0.25

Table 1: Mass and Composition of VSV Subviral Particles

component	copies per virion	monomer mass (MDa)	mass per virion (MDa)	percent of total protein	source
RNA	1 × 11000 bases		3.7		
N protein	1300	0.047	59.6	33.0	*a*
L protein	50	0.242	12.1	6.7	*a*
P protein	466	0.025	11.7	6.5	*a*
nucleocapsid			87.1	46.0	
M protein	2,000	0.026	52.0	30.0	*b*
nucleocapsid-M protein complex			139	76.0	*b*
G protein	710	0.062	44.0	24.0	*b*
lipid			56.0		*a*
virion total			239		

[a] Thomas et al. (1985). [b] Values for M protein and G protein were calculated from the mass of the nucleocapsid determined by Thomas et al. (1985) and a determination of an M/N weight ratio = 0.90 and G/N ratio = 0.73 for the virus preparations used in the present study. These values differ slightly from those published by Thomas et al. (M/N = 0.80 and G/N = 1.12) probably due to minor differences in virus strain or culture conditions.

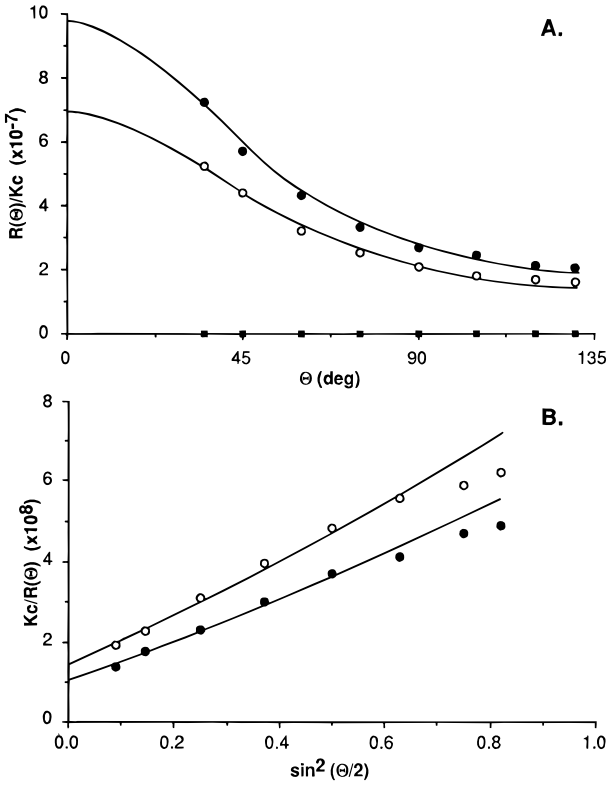

FIGURE 1: Angular dependence of light scattering intensity from VSV nucleocapsids. Closed circles: Nucleocapsids released from virions by solubilization of the envelope in buffer containing 250 mM NaCl and 0.1% Triton X-100. Closed squares: Supernatant from the same sample following removal of the nucleocapsids by ultracentrifugation. Open circles: Nucleocapsids purified by sucrose gradient centrifugation. Solid curves: Nonlinear least-squares fit to shape function for a random coil. (A) Plot of intensity [$R(\Theta)$] normalized for nucleocapsid protein concentration (c) and experimental constants (K) versus detector angle relative to the light path (Θ). (B) Plot of reciprocals of the data in panel A versus $\sin^2(\Theta/2)$.

M NaCl, and light scattering intensity was determined as a function of detector angle (Figure 1A, closed circles). The data shown are intensities [$R(\Theta)$, background subtracted and normalized to a standard] divided by protein concentration (c) and a proportionality constant (K) that depends on experimental constants (light wavelength, refractive index of solvent, refractive index increment of protein). The light scattering intensity displayed a marked angular dependence and was >7-fold above the background from a buffer blank containing Triton X-100, even at the largest angle examined (130°). The viral nucleocapsids were removed by ultracentrifugation. The resulting supernatant contained 90−95% of the M protein and all of the G protein as determined by SDS−PAGE (not shown), consistent with previous data (Kaptur et al., 1991; McCreedy et al., 1990). The supernatant displayed little or no light scattering intensity above that of the buffer blank (Figure 1A, closed squares), indicating that light scattering following solubilization of the virion envelope was attributable almost entirely to nucleocapsids. Therefore, the protein concentration (c) used in the calculation of $R(\Theta)/Kc$ for nucleocapsids was routinely determined using virions labeled with [^{35}S]methionine. The radioactivity before and after ultracentrifugation was used to calculate the protein concentration due to nucleocapsids.

Nucleocapsids purified from solubilized envelope components by sucrose gradient centrifugation (open circles) showed a similar angular dependence of light scattering intensity, but the intensities were slightly less than those of unpurified nucleocapsids. This was probably due to fragmentation of some of the nucleocapsids and the loss of some of the P and L protein during isolation as described previously (Thomas et al., 1985), leading to a slightly lower average molecular mass.

The value of $R(\Theta)/Kc$ extrapolated to $\Theta = 0°$ is a measurement of the molecular mass of the viral nucleocapsid (M_{NC}). The value of $R(\Theta)/Kc$ at any angle is given by $M_{NC}P(\Theta)$, where $P(\Theta)$ is an angle-dependent shape function that depends on the shape of the scattering particle and its size (radius of gyration, R_G) relative to the wavelength of the light being scattered. $P(\Theta)$ varies from a value of 1 at $\Theta = 0°$ to a value of 0 at large angles for particles much larger than the wavelength of scattered light. In electron micrographs the VSV nucleocapsid appears to be flexible enough to resemble a random coil (e.g., Heggeness et al., 1980; Newcomb & Brown, 1981; Newcomb et al., 1982; Thomas et al., 1985). Therefore, the data in Figure 1A were fit to the shape function for a random coil using a nonlinear least-squares fit of two parameters, M_{NC} and R_G (Figure 1A, solid curves). For unpurified nucleocapsids (closed circles), M_{NC} = 97.5 MDa and R_G = 173 nm, and for purified nucleocapsids (open circles), M_{NC} = 69.5 MDa and R_G = 164 nm. Repeated determinations using several different virus preparations gave $M_{NC} = 87.5 \pm 22.5$ MDa and $R_G = 178 \pm 35$ nm (mean ± SD, $N = 7$). Most of the variability was due to variation between virus preparations, while repeated determinations on a single virus preparation gave a higher degree of precision. The value of M_{NC} for purified nucleocapsids is in good agreement with the value of 69.4 MDa determined by scanning tunneling electron microscopy (Thomas et al., 1985) and that of the unpurified nucleocapsids is in good agreement with the value of 87.1 MDa calculated from its composition (Table 1).

Figure 1B shows a plot of $Kc/R(\Theta)$ versus $\sin^2(\Theta/2)$ for the data in Figure 1A. Such a plot is usually used to linearize angle-dependent light scattering data to determine 1/molecular mass from the y-intercept. The theoretical basis for this analysis is valid only for particles which are relatively small compared to the wavelength of scattered light such that the angular dependence is small. Even though this is clearly

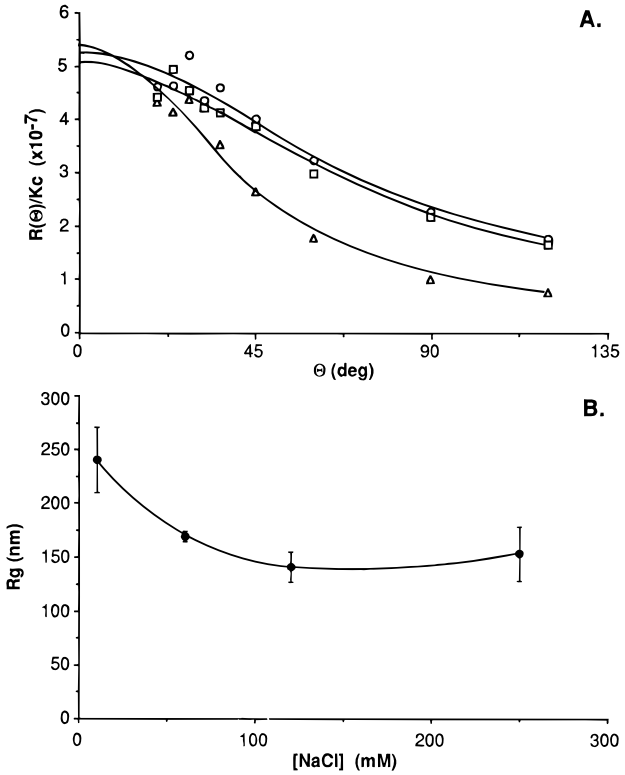

FIGURE 2: Angular dependence of light scattering intensity from purified VSV nucleocapsids as a function of NaCl concentration. (A) Plot of intensity [$R(\Theta)$] normalized for nucleocapsid protein concentration (c) and experimental constants (K) versus detector angle (Θ) for purified nucleocapsids in buffer containing NaCl at 10 mM (triangles), 120 mM (circles), or 250 mM (squares). Solid curves: nonlinear least-squares fit to shape function for a random coil. (B) Plot of radius of gyration (R_G) of purified nucleocapsids determined by nonlinear least-squares fit of the data in panel A. Data obtained at 60 mM NaCl were not shown in panel A for clarity of presentation.

not the case for the present data, the scattering function for a random coil approximates a straight line in this size range (solid curves). Presentation of the data in the reciprocal form (Figure 1B) shows that at larger angles the data deviate from the fitted curve obtained by the nonlinear least-squares fit from Figure 1A. This deviation is more pronounced for the purified nucleocapsids (open circles) and provides further evidence for heterogeneity in the size of the nucleocapsids, since the presence of smaller nucleocapsids has more influence at larger angles. An alternative explanation is that the nucleocapsids deviate slightly from the behavior of a random coil. Interpolation to $\Theta = 0$ by a linear least-squares fit of the data in Figure 1B gave values for the molecular mass of the nucleocapsids that were slightly less than those obtained by the nonlinear least-squares fit of the data in Figure 1A. This is due to the greater weight given by the reciprocal data (Figure 1B) to the data points from larger angles.

Salt-Dependent Changes in the Conformation of Nucleocapsids. Figure 2A shows the angular dependence of light scattering by purified nucleocapsids at NaCl concentrations of 10 mM (triangles), 120 mM (circles), and 250 mM (squares). At each detector angle the intensity of scattered light was greatest at 120 mM NaCl and least at 10 mM. The data were analyzed by the nonlinear least-squares fit used in Figure 1A (solid curves). The salt-dependent changes in light scattering intensity were due to changes in radius of

Table 2: Molecular Weights of Nucleocapsids Determined at Different Protein Concentrations and Ionic Strengths[a]

NaCl concentration (mM)	protein concentration (μg/mL)			
	12[b]	9[b]	6[b]	3[b]
10	6.34 ± 1.64	5.85 ± 1.33	5.62 ± 0.83	6.35± 0.47
60	6.25 ± 1.36	6.09 ± 1.07	5.52 ± 0.87	6.02 ± 0.40
120	5.63 ± 1.13	5.99 ± 1.36	6.28 ± 0.72	6.51 ± 0.097
250	5.33 ± 0.88	5.89 ± 1.22	5.95 ± 1.26	5.94 ± 0.83

[a] Purified nucleocapsids in buffer at the indicated protein concentrations were shifted to the indicated final NaCl concentration, and light scattering intensity was recorded as a function of detector angle. The intensity data similar to those in Figure 2 were fit to the shape function for a random coil using a nonlinear least squares fit of two parameters, molecular weight and radius of gyration. The data are the means ± SD for three different nucleocapsid preparations. [b] Molecular weight ($\times 10^{-7}$).

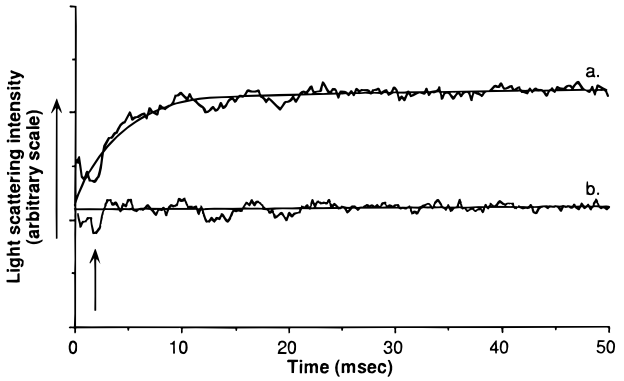

FIGURE 3: Stopped-flow analysis of conformational changes in purified VSV nucleocapsids upon shift in NaCl concentration. Curve a: Nucleocapsids in buffer containing 10 mM NaCl shifted to 120 mM NaCl (final concentration). Smooth curve: nonlinear least-squares fit to a single exponential. Curve b: Nucleocapsids in buffer containing 10 mM NaCl mixed with the same buffer. Arrow indicates mixing time of the stopped-flow instrument.

gyration rather than to changes in molecular mass, since the curves intersect the y-axis at similar values. The values for R_G obtained at different salt concentrations are shown in Figure 2B. These changes in R_G correspond to salt-dependent conformational changes in the nucleocapsid that have been observed by electron microscopy (Heggeness et al., 1980).

In the experiment shown in Figure 2, additional data were collected at lower angles (20−35°) than in the experiment in Figure 1 to provide more data near the y-intercept to test the validity of the extrapolation. Even though there was more experimental variation at angles <35°, the extrapolated values of the y-intercepts were not changed significantly if these data were not included in the fit. The light scattering changes seen in Figure 2A were not affected by potential salt-dependent changes in intermolecular interactions, since the value for the molecular mass was independent of protein concentration (Table 2).

Figure 3 shows the time course of the conformational change in VSV nucleocapsids upon shifting the salt concentration from 10 to 120 mM NaCl determined by stopped-flow analysis (curve a). The rapid reaction time was close to the mixing time of the instrument (approximately 2 ms, indicated by the arrow). However, the data were free of mixing artifacts after 2 ms as shown by a control in which the salt concentration was not shifted (curve b). These data were fit to a single exponential (smooth curve) and gave a

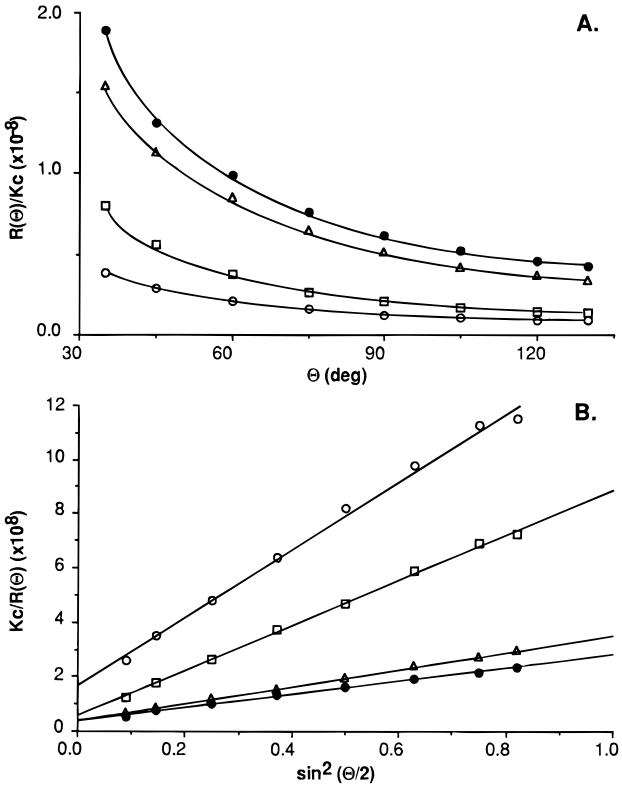

FIGURE 4: Angular dependence of light scattering intensity from VSV NCM complexes as a function of NaCl concentration. (A) Plot of intensity [$R(\Theta)$] normalized for protein concentration (c) of NCM complexes and experimental constants (K) versus detector angle (Θ) for NCM complexes released from virions by solubilization of the envelope in buffer containing 0.1% Triton X-100 and NaCl at 10 mM (closed circles), 60 mM (triangles), 120 mM (squares), or 250 mM (open circles). (B) Plot of reciprocals of the data in A versus $\sin^2(\Theta/2)$. Solid lines: Linear least squares fit of the data.

rate constant of 234 s^{-1} ($t_{1/2}$ = 3.0 ms). This rate was independent of salt concentration (not shown). In repeated experiments, the rate was determined to be 260 ± 90 s^{-1} (mean ± SD, N = 9).

Intensity and Angular Dependence of Light Scattering by NCM Complexes. VSV virions were solubilized with Triton X-100 in varying concentrations of NaCl in order to vary the amount of M protein associated with nucleocapsids. Light scattering intensity was determined as a function of detector angle (Figure 4A). As expected, the light scattering intensities of the NCM complexes displayed a marked angular dependence, similar to that of nucleocapsids (Figure 1A). In addition, the light scattering intensities at each detector angle were very sensitive to the amount of M protein bound to the nucleocapsid. Since the intact NCM complex is a tightly coiled, bullet-shaped particle, it would be inappropriate to fit the angular dependence data in Figure 4A to the shape function for a random coil, as in the case of nucleocapsids without M protein (Figure 1A). This is also true for NCM complexes from which some of the M protein has dissociated, which probably have a mixture of coiled and uncoiled regions (Newcomb et al., 1982; Odenwald et al., 1986). Similar to the case of nucleocapsids without M protein (Figure 1B), the empirical observation was made that a plot of $Kc/R(\Theta)$ versus $\sin^2(\Theta/2)$ for the NCM complexes approximated a straight line (Figure 4B). Thus the apparent molecular mass [$R(\Theta)/Kc$ at $\Theta = 0°$] could be approximated

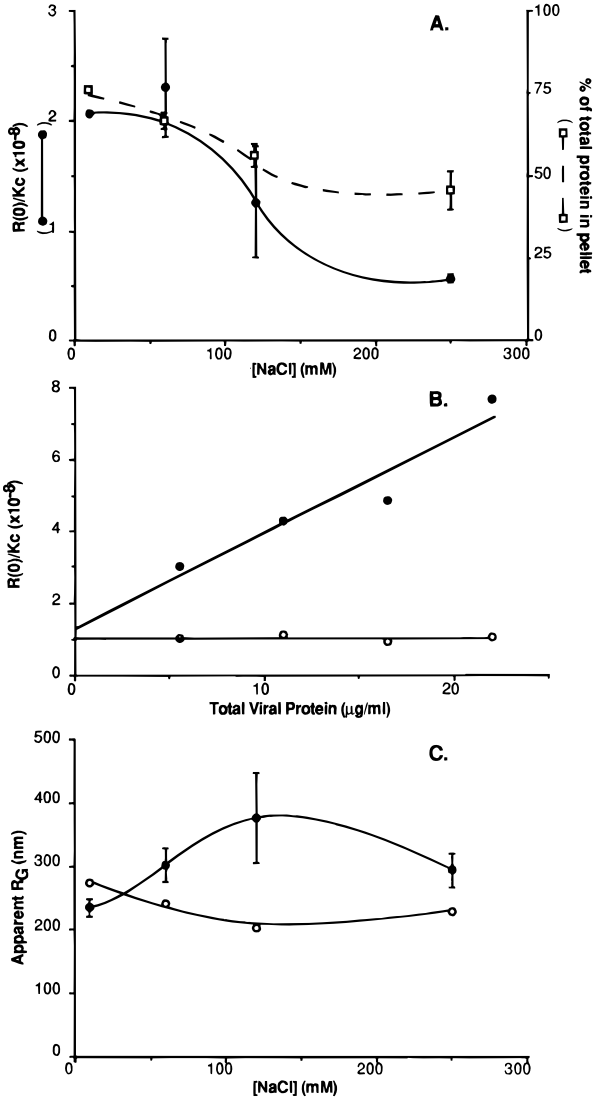

FIGURE 5: Apparent molecular mass and R_G of NCM complexes. (A) Virions were solubilized in buffer containing 0.1% Triton X-100 and the indicated NaCl concentration. Data shown (closed circles) are light scattering intensities extrapolated to $\Theta = 0°$ [$R(0)/Kc$] by linear least-squares analysis of data similar to those in Figure 4B. Open squares are the percent of total viral protein in NCM complexes determined from the amount of protein in the pellet after ultracentrifugation. (B) Concentration dependence of molecular mass of nucleocapsids and NCM complexes. Virions at the indicated protein concentrations were solubilized in buffer containing 0.1% Triton X-100 and NaCl at 10 mM to release NCM complexes (closed circles) or 250 mM to release nucleocapsids (open circles). Data shown are light scattering intensities extrapolated to $\Theta = 0°$ [$R(0)/Kc$] by linear least-squares analysis of data similar to those in Figure 4B. (C) Apparent R_G of NCM complexes (closed circles) were calculated from the ratio of the slope to the intercept of linear least-squares analysis of data similar to those in Figure 4B. A similar analysis of the data from Figure 2 is shown for purified nucleocapsids lacking M protein (open circles).

from the reciprocal of the y-intercept, and an apparent R_G could be calculated from the slope/y-intercept.

The apparent molecular mass was calculated from data similar to those in Figure 4 for NCM complexes at different salt concentrations (Figure 5A, closed circles). The changes in apparent molecular mass at increasing salt concentrations generally paralleled the extent of M protein binding as reflected in the fraction of total viral protein that could be pelletted by ultracentrifugation (Figure 5A, open squares). In fact, the decrease in light scattering intensity upon

dissociation of M protein was greater than that expected based on the change in molecular mass alone. For example, in the data in Figure 5A, the theoretical change in molecular mass of the NCM complex between 10 and 250 mM NaCl would be about 40% (from 76% of total viral protein to 46%), while the value of $R(\Theta)/Kc$ at most angles was actually reduced by 70−80%. Thus, additional factors contributed to these changes in scattering intensity.

Virions at different protein concentrations were solubilized with Triton X-100 in the presence of 10 mM NaCl, in order to evaluate the extent of self-association of the NCM complex. The angular dependence of light scattering intensity was determined as in Figure 4A. The NaCl concentration was then raised to 250 mM in order to dissociate M protein, and the light scattering measurements were repeated. The apparent molecular mass [$R(0)/Kc$] of the nucleocapsids and NCM complexes was determined from the reciprocal of the y-intercepts of plots similar to those in Figure 4B and are shown in Figure 5B. The apparent molecular mass of the NCM complex (closed circles) increased as a function of concentration, while that of the nucleocapsid (open circles) remained constant. These data indicate that the NCM complexes self-associate over the concentration range examined, while nucleocapsids lacking M protein do not. The self-association of NCM complexes in this concentration range was reversible, as shown by a decrease in molecular mass when complexes formed at high protein concentration were diluted to low concentration (data not shown). Extrapolation of the molecular mass of the NCM complex to zero protein concentration gave a value of 129 MDa, in good agreement with the theoretical monomer molecular mass of 135 MDa (Table 1). Depending on the individual preparation, in the typical concentration range used for most of the light scattering analyses (approximately 10 μg/mL total protein), the molecular mass of the NCM complexes was 2- (Figure 5A) to 3-fold (Figure 5B) that of the monomer, while that of nucleocapsids without M protein was very close to the monomer molecular mass. Thus changes in the degree of self-association contributed to the changes in light scattering intensity upon dissociation of M protein from the NCM complex in experiments such as that in Figure 4.

The apparent R_G calculated for NCM complexes at different salt concentrations is shown in Figure 5C (closed circles) together with a similar analysis of the data for purified nucleocapsids lacking M protein from Figure 2 (open circles). The values for R_G calculated by this method differ slightly from those calculated by nonlinear least-squares fit to the shape function for a random coil (Figure 2B), presumably because of the differences in underlying assumptions in each analysis. The NCM complexes underwent conformational changes that gave rise to changes in apparent R_G at the same salt concentrations as nucleocapsids lacking M protein (Figure 5C); however, the changes were in opposite directions. The maximum R_G for NCM complexes was obtained at 120 mM NaCl, which gave the minimum R_G for nucleocapsids lacking M protein. These data indicate that, upon dissociation of M protein, NCM complexes undergo conformational changes that contribute to the decreased light scattering intensity at increasing salt concentrations up to 120 mM NaCl. However, at 250 mM NaCl, the R_G of the nucleocapsid was similar to that of the intact NCM complex at 10 mM NaCl, even though the shapes are quite different. Thus little of the difference in light scattering intensity at these two salt concentrations can be attributed to the change in shape.

Dynamic Light Scattering Analysis of Nucleocapsids and NCM Complexes. The difference in extent of self-association between nucleocapsids and NCM complexes was confirmed by analysis of their translational diffusion by photon correlation spectroscopy (dynamic light scattering). Virions at different protein concentrations were solubilized with Triton X-100 in the presence of 10 mM NaCl. The photon-count autocorrelation function was determined at varying detector angles. The NaCl concentration was then raised to 250 mM in order to dissociate M protein, and the light scattering measurements were repeated. Figure 6A shows the data for nucleocapsids (open circles) and NCM complexes (closed circles) obtained at a detector angle of 90° and a concentration of 13 μg/mL total protein. The data shown are the intensity-normalized autocorrelation functions [$C'(t)$] calculated by dividing the value in each correlator channel [$C(t)$] by the baseline (uncorrelated) value determined from the average of six correlator channels with long delay times. $C'(t)$ of nucleocapsids decayed more rapidly than that of NCM complexes. This difference could be due to several factors such as faster diffusion (smaller Stokes radius) or greater intramolecular flexibility of nucleocapsids compared to NCM complexes.

The data from experiments similar to those in Figure 6A were fit to an exponential decay (solid curves) using second-order cumulants analysis (Koppel, 1972), which gives an average rate constant Γ and a second moment to account for the distribution of particle sizes. Since $\Gamma = D_t(4\pi n_0/\lambda_0)^2 \sin^2(\Theta/2)$, the translational diffusion coefficient, D_t, can be calculated from the slope of a plot of Γ versus $\sin^2(\Theta/2)$. Figure 6B shows such a plot for nucleocapsids (open circles) and NCM complexes (closed circles) at a concentration of 13 μg/mL total protein. The data for NCM complexes were fit well by a linear least-squares analysis, and D_t was calculated from the slope. However, the data for nucleocapsids were distinctly nonlinear. Similar nonlinearity was observed over a 4-fold concentration range (4.25−17 μg/mL total viral protein), indicating that it arises from intramolecular effects. Such deviation from linearity at high angles can arise either from intramolecular flexibility or from a significant contribution due to rotational diffusion (Palmer & Fritz, 1979). In either case, translational diffusion is the dominant factor at low angles. Therefore D_t for nucleocapsids was calculated only from the data obtained at 45° and 60°.

The values for D_t together with the solvent viscosity and temperature were used to calculate the Stokes radii, R_S, for NCM complexes (Figure 6C) and nucleocapsids (Figure 6D) and are shown as a plot of R_S versus protein concentration. The R_S of the NCM complex (Figure 6C) increased as a function of concentration, while that of the nucleocapsid (Figure 6D) remained constant. These data support the conclusion drawn from the concentration dependence of light scattering intensity (Figure 5) that the NCM complexes self-associate over the concentration range examined, while nucleocapsids lacking M protein do not. Extrapolation of the data in Figure 6C,D to zero protein concentration gave $R_S = 65$ nm for a monomer NCM complex and $R_S = 86$ nm for nucleocapsids.

Kinetics of Light Scattering Intensity Changes upon Dissociation of M Protein from NCM Complexes. The data

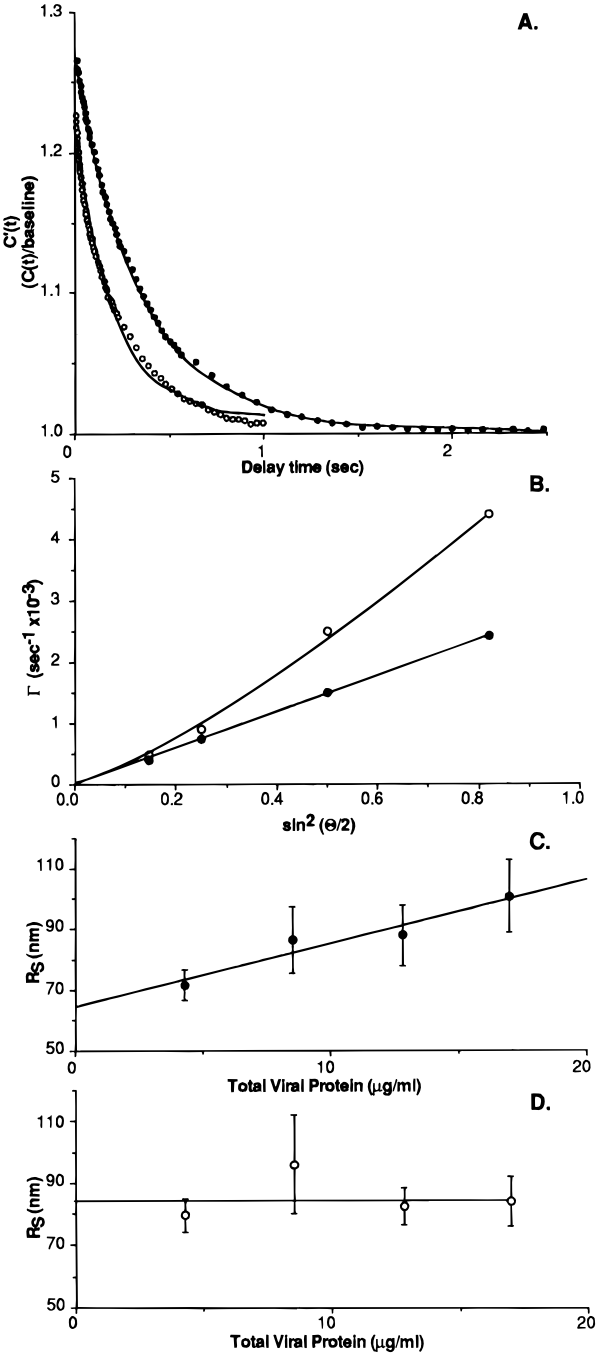

FIGURE 6: Dynamic light scattering analysis of VSV nucleocapsids and NCM complexes. (A) Intensity-normalized autocorrelation functions [$C'(t)$] calculated by dividing the value in each correlator channel [$C(t)$] by the baseline (uncorrelated) value determined from the average of six correlator channels with long delay times. Data for nucleocapsids (open circles) and NCM complexes (closed circles) obtained by solubilization of virion envelopes in buffer containing 0.1% Triton X-100 and either 10 mM NaCl (NCM complexes) or 250 mM NaCl (nucleocapsids) at a detector angle of 90° and a concentration of 13 μg/mL total virion protein. Solid curves: Least-squares fit of the data by second order cumulants analysis. (B) Plot of average rate constant Γ for decay of autocorrelation functions versus $\sin^2(\Theta/2)$ determined from data similar to those in panel A. (C) Concentration dependence of Stokes radius (R_S) for NCM complexes calculated from the slope obtained from data similar to those in panel B. (D) Concentration dependence of Stokes radius (R_S) for nucleocapsids calculated from the data obtained at 45° and 60° detector angles.

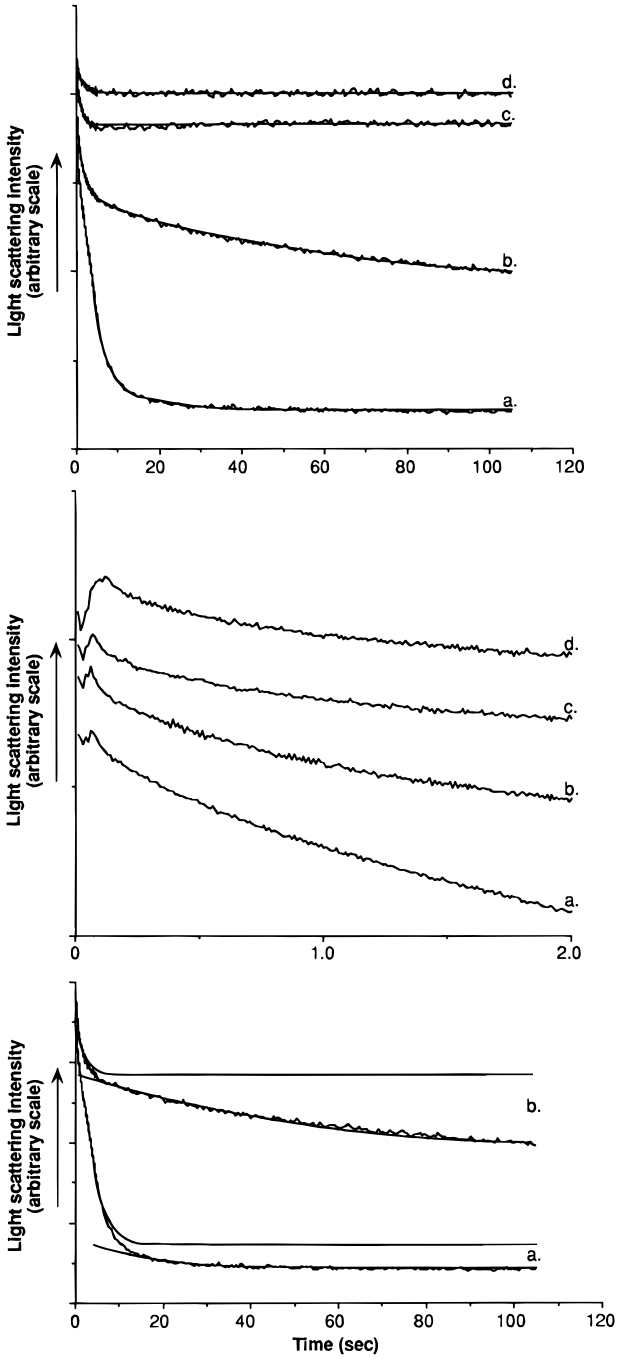

FIGURE 7: Stopped-flow analysis of the light scattering intensity changes accompanying dissociation of M protein from VSV NCM complexes. (A) NCM complexes in buffer containing 0.1% Triton X-100 and 10 mM NaCl shifted to final NaCl concentrations of 250 mM (a), 120 mM (b), 60 mM (c), or 40 mM (d). Smooth curves: Nonlinear least-squares fit to one exponential (c, d) or two exponentials (a, b). (B) Data in panel A are expanded to show the initial 2 s. (C) Data in panel A (curves a and b) with smooth curves to illustrate two exponentials separately.

in Figures 4−6 indicate that three factors contribute to changes in light scattering intensity upon dissociation of M protein from the NCM complex at increasing salt concentrations: (1) the change in molecular mass and protein concentration contributed by M protein, (2) the change in conformation of the NCM complexes, and (3) the change in extent of self-association of the NCM complexes. As shown in Figure 7, these three factors can be distinguished kinetically as well as by analysis of angular dependence under equilibrium conditions. Figure 7A shows stopped-flow analysis of the changes in light scattering intensity at $\Theta = 90°$ for NCM complexes upon shifting the NaCl concentra-

Table 3: Rate Constants for Changes in Light Scattering Intensity upon Dissociation of NCM Complexes as a Function of NaCl Concentration

NaCl concentration (mM)	k_1 (s^{-1}) (mean ± SD)	k_2 (s^{-1}) (mean ± SD)	N
40	0.700 ± 0.122		8
60	0.869 ± 0.129		8
120	0.529 ± 0.080	0.020 ± 0.006	8
250	0.437 ± 0.101	0.049 ± 0.020	9

[a] NCM complexes in buffer containing 10 mM NaCl were shifted to the indicated final NaCl concentration, and light scattering intensity was recorded as a function of time for 105 s in a stopped-flow apparatus. The data from 0.4 to 105 s were fit to either to a single exponential, $I(t) = I_1e^{-k_1t} + I_f$, or to a double exponential, $I(t) = I_1e^{-k_1t} + I_2e^{-k_2t} + I_f$, by a nonlinear least-squares fit of three parameters (I_1, k_1, I_f) or five parameters (I_1, k_1, I_2, k_2, I_f), respectively.

tion from 10 to 250 mM (curve a), 120 mM (curve b), 60 mM (curve c), or 40 mM (curve d). The changes in light scattering intensity in Figure 7A actually occur in three phases. Figure 7B illustrates the fastest phase by expanding the time scale to include the initial 2 s. Prior to the decrease in light scattering intensity that accompanied dissociation of M protein, there was a small, rapid increase in light scattering intensity of the NCM complex that occurred during the initial 100−200 ms following the shift in NaCl concentration. This is reminiscent of the conformational changes that occurred in purified nucleocapsids without M protein upon shifting the NaCl concentration (Figure 3) and appears to correspond to similar conformational changes in the NCM complex.

The decrease in light scattering intensity that followed the small initial increase was analyzed by nonlinear least-squares fit of the data to an exponential decay beginning at the 400 ms time point (smooth curves in Figure 7A). The data obtained at 60 and 40 mM NaCl (curves c and d) were fit well by single exponentials with rate constants of 1.0 and 0.6 s^{-1} respectively. There was no significant improvement by fitting the data to two exponentials. However, the data obtained at 250 and 120 mM NaCl (curves a and b) could not be adequately fit by single exponentials but were fit well by assuming two exponential decays. Figure 7C shows the theoretical time courses of the two exponentials (smooth curves) together with the original data. The rate constants for the rapid phases were 0.4 and 0.6 s^{-1} at 250 mM (a) and 120 mM NaCl (b), respectively, while those of the slow phases were 0.06 and 0.02 s^{-1}.

Most of the changes in light scattering intensity occurred in the rapid phase. The rapid phase directly reflected the changes in molecular weight due to dissociation of M protein, while the slow phase reflected the decrease in extent of self-association of the NCM complex. This was shown by the fact that the magnitude of the change in intensity in the rapid phase corresponded to the amount of M protein that dissociated at each NaCl concentration (i.e., 250 mM > 120 mM > 60 mM > 40 mM). In contrast, the magnitude of the slow phase was greater at 120 mM NaCl than at 250 mM (Figure 7C). Furthermore, the magnitude of the rapid phase was relatively insensitive to changing protein concentration, while the magnitude of the slow phase was markedly dependent on protein concentration (data not shown) and usually could not be detected below a concentration of 5−10 μg/mL total viral protein, indicating that the magnitude of the slow phase reflected the extent of self-association of the NCM complex. Table 3 summarizes the rate data obtained at different NaCl concentrations in repeated experiments similar to that in Figure 7. Table 4 summarizes the rate data obtained at different protein concentrations. These data indicate that the stopped-flow light scattering technique can be used to analyze the binding constants and rate constants for association of M protein with nucleocapsids under a variety of experimental conditions and that the rate of M protein dissociation from the NCM complex is not affected significantly by the self-association of the NCM complexes under these conditions.

Table 4: Rate Constants for Changes in Light Scattering Intensity upon Dissociation of NCM Complexes at Different Protein Concentrations

total viral protein (mg/mL)	k_1 (s^{-1}) (mean ± SD)	N
30	0.283 ± 0.095	9
15	0.311 ± 0.099	14
7.5	0.331 ± 0.089	12
3.8	0.250 ± 0.070	16
1.9	0.228 ± 0.049	10

[a] NCM complexes in buffer containing 10 mM NaCl were shifted to a final NaCl concentration of 250 mM and the indicated final protein concentration. Light scattering intensity was recorded as a function of time for 105 s in a stopped-flow apparatus. The data from 0.4 to 105 s were fit to either a single exponential, $I(t) = I_1e^{-k_1t} + I_f$, or to a double exponential, $I(t) = I_1e^{-k_1t} + I_2e^{-k_2t} + I_f$, by a nonlinear least squares fit of 3 parameters (I_1, k_1, I_f) or 5 parameters (I_1, k_1, I_2, k_2, I_f), respectively. The data obtained at 7.5, 3.8, and 1.9 μg/mL were fit equally well by single or double exponential fits, while the data obtained at 30 and 15 μg/mL were fit significantly better by a double exponential.

DISCUSSION

The data presented here have established criteria for light scattering analysis of the interaction of M protein with nucleocapsids, which has significant advantages over previously described techniques. Three factors have been identified that contribute to the light scattering properties of VSV nucleocapsids: the nucleocapsid conformation, the extent of self-association, and the amount of bound M protein. All three of these factors were affected by changes in ionic strength. However, they could be distinguished as follows. Conformational changes in nucleocapsids and NCM complexes were reflected in changes in the angular dependence of light scattering intensity (i.e., changes in R_G) and occurred rapidly (millisecond time scale) upon changing salt concentration. Changes in extent of self-association could be distinguished by the concentration dependence of the apparent molecular mass and diffusion coefficient of the NCM complex and occurred relatively slowly (seconds to minutes time scale). Changes in M protein binding were reflected in changes in both molecular mass and R_G and occurred on an intermediate time scale ($t_{1/2}$ approximately 1 s).

The conformation of the helical VSV nucleocapsid changes reversibly as a function of salt concentration even in the absence of M protein. These changes are visible by electron microscopy as changes in the spacing between coils of the helix and in the apparent flexibility of the helix (Heggeness et al., 1980). Similar changes occur in the nucleocapsids of the structurally similar paramyxoviruses and probably in those of other viruses with helical nucleocapsids (Heggeness et al., 1982b). Although the salt-dependent changes in conformation of the VSV nucleocapsid have only been

characterized previously at two NaCl concentrations by electron microscopy (Heggeness et al., 1980), the changes in angular dependence of light scattering intensity observed here for VSV nucleocapsids correlate well with the changes observed by electron microscopy of paramyxovirus nucleocapsids at a wider variety of NaCl concentrations in the same study. At low salt concentration, the nucleocapsid helix is loosely coiled and appears to be sufficiently flexible to resemble a random coil. Since R_G is related to the end-to-end distance for a random coil (Marshall, 1978), this corresponds to the maximum R_G. At physiological salt concentrations, the spacing of the helical coils is tighter (which reduces the overall length), but the nucleocapsid retains its apparent flexibility. This corresponds to the minimum R_G at 120 mM NaCl. At high salt concentration, the helix is also more tightly coiled, but the nucleocapsid appears to be less flexible, giving rise to a larger R_G than at 120 mM NaCl. However, even at high salt concentrations, nucleocapsids lacking M protein are not condensed into the tightly coiled, bullet-shaped structure that is characteristic of the NCM complex.

Even though nucleocapsids probably do not experience changes in salt concentration in infected cells *in vivo*, the ability of the nucleocapsid to undergo rapid conformational changes on the millisecond time scale as shown here is probably relevant to its function *in vivo*. For example, condensation of the nucleocapsid following M protein binding probably occurs on the cytoplasmic surface of the host plasma membrane *in vivo* (Odenwald et al., 1986). Based on the data presented here, the condensation step is likely to occur rapidly relative to the rate of M protein binding. This idea is supported by stopped-flow analysis of light scattering by NCM complexes upon shifting to higher salt concentrations (Figure 7), which is essentially the reverse of the M protein binding and condensation that occurs in the assembly process. In this case, the dissociation of M protein was preceded by small increases in light scattering intensity consistent with rapid conformational changes in the NCM complex.

Conformational differences between nucleocapsids and NCM complexes were also apparent at equilibrium after shifting the salt concentration as shown by greater angular dependence of light scattering intensity (larger R_G) for NCM complexes compared to purified nucleocapsids (Figure 5C). These differences were more pronounced at intermediate salt concentrations, in which the NCM complexes probably consist of a mixture of coiled and uncoiled regions (Newcomb et al., 1982; Odenwald et al., 1986). Surprisingly, the intact NCM complex at 10 mM NaCl and nucleocapsids from which the M protein had dissociated at 250 mM did not differ markedly in angular dependence of light scattering intensity (Figure 5C) despite the dramatic differences in shape determined by electron microscopy (Newcomb & Brown, 1981; Newcomb et al., 1982). This probably reflects the fact that in solution, the nucleocapsid "random coil" is similar in size to the condensed bullet-like NCM complex. This idea is supported by the observation that monomer forms of the nucleocapsid and NCM complex had similar Stokes radii as determined by dynamic light scattering analysis (Figure 6C,D).

One of the concerns about biochemical analysis of viral M proteins and M protein-containing structures such as NCM complexes is their pronounced tendency to aggregate. This tendency was apparent in the present study by the concentration dependence of the molecular mass (Figure 5B) and Stokes radii (Figure 6C) of NCM complexes under conditions where nucleocapsids lacking M protein remained monomeric. At the concentrations used for most of the analyses presented here (approximately 10 μg/mL total viral protein), the average molecular mass of the NCM complex was 2−3-fold greater than the monomer molecular mass determined by extrapolation to zero protein concentration (Figure 5). Since light scattering analysis gives a weight-average molecular mass, the average state of aggregation of the NCM complexes (arithmetic mean) would be somewhat less, indicating that the NCM complexes existed primarily as mixtures of monomers, dimers, and trimers.

Solubilization of virion envelopes at high protein concentrations (around 1 mg/mL) and isolation of NCM complexes by sedimentation in sucrose gradients similar to the procedure for purification of nucleocapsids resulted in preparations that were highly aggregated (molecular mass >10-fold that of monomer) in which reversal of aggregation occurred slowly if at all (unpublished results). However, at the lower protein concentrations used here, the self-association of NCM complexes was reversible. For example, the dissociation of nucleocapsids or NCM complexes from each other was apparent as a separate phase in the kinetics of light scattering changes following shift in salt concentration from 10 mM to either 120 or 250 mM NaCl (Figure 7C). Reversal of self-association was also apparent as a time-dependent reduction in light scattering intensity upon dilution of NCM complexes to lower protein concentrations (unpublished results). Thus the ability to analyze the properties of NCM complexes immediately after solubilization of the virion envelope without further purification represents a significant advantage of the light scattering approach.

Of course, the major advantage of light scattering analysis of NCM complexes is its sensitivity to the amount of M protein bound to the nucleocapsid. This arises from two factors. The first is the change in molecular mass. For example, complete dissociation of M protein from the intact NCM complex should reduce the molecular mass to 65% of its original value (from 135 to 87.1 MDa, Table 1). The second is the change in protein concentration that effectively contributes to light scattering. Since the soluble M protein is a 0.026 MDa monomer (McCreedy et al., 1990), it makes no significant contribution to light scattering compared to the nucleocapsid. Thus the effective protein concentration is also reduced to 65% of its initial value by dissociation of M protein, so that in theory light scattering intensity should be reduced by a factor of 0.42 (0.65^2). In fact, the reduction is somewhat greater due to the changes in shape and self-association that accompany dissociation of M protein. Nonetheless, the changes in light scattering intensity upon shifting the salt concentration were dominated by the change in molecular mass and effective protein concentration (Figure 7), which is a direct measure of M protein binding.

The kinetics of M protein binding were readily resolved from those of the changes in conformation and self-association, which were more than an order of magnitude faster and slower, respectively. The $t_{1/2}$ of the light scattering changes due to dissociation of M protein after shifting the salt concentration ($\ln 2/k_1$, Table 2) ranged from 0.8 s at 60 mM NaCl to 1.6 s at 250 mM NaCl. These values were relatively insensitive to changes in experimental parameters

such as pH (in the range from pH 5 to 8) or type of detergent (unpublished results). Importantly, they were not affected by the extent of self-association of the NCM complex observed at the protein concentrations studied here (2−30 μg/mL total viral protein, Table 4). However, they were markedly affected by loss of the native structure of the M protein-nucleocapsid interaction, e.g., by prolonged storage of virions, which usually resulted in much slower dissociation of M protein (unpublished results).

It might be expected that the rate constants for M protein dissociation from the NCM complex would vary considerably at different salt concentrations. However, it was found that these rate constants only varied by a factor of 2-fold between 40 and 250 mM NaCl, with the slowest rate constants observed at 250 mM NaCl (Table 2). One possible explanation would be that the NCM complex contains different populations of M protein molecules that differ in the salt sensitivity of their association with the nucleocapsid but which dissociate at similar rates (multiple types of sites, nonreversible binding). Another possibility is that the binding of M protein to the nucleocapsid is a dynamic equilibrium in which the dissociation constant varies with ionic strength. In this case, the rate constant for the approach to equilibrium after shifting the salt concentration contains contributions from both the forward and reverse reactions (i.e., both dissociation and rebinding of M protein), similar to the case in temperature-shift and other perturbation experiments. Additional salt-shift and subunit exchange experiments have shown that this latter explanation is correct (manuscript in preparation).

In summary, the data presented here provide criteria for assessing binding of the VSV M protein to nucleocapsids under conditions of minimal perturbation of the NCM complex assembled *in vivo*. This was accomplished by light scattering analysis of nucleocapsids and NCM complexes immediately after solubilization of the envelope without further manipulation. The sensitivity of the light scattering technique allowed the analysis to be performed at low protein concentrations so that self-association of the NCM complex was minimal and reversible. Under these conditions the nucleocapsid and NCM complex were observed to undergo conformational changes within milliseconds followed by dissociation of M protein within seconds after shifting the salt concentration. These results suggest that similar rapid changes in M protein binding and nucleocapsid conformation can also occur *in vivo*. These data indicate that light scattering techniques can be used to analyze the interaction of M protein with nucleocapsids such as determination of binding constants and rate constants and the effects of mutations in viral genes on association of M protein with nucleocapsids.

REFERENCES

Atkinson, P. H., Moyer, S. A., & Summers, D. F. (1976) *J. Mol. Biol. 102*, 613−631.
Barge, A., Gaudin, Y., Coulon, P., & Ruigrok, R. W. H. (1993) *J. Virol. 67*, 7246−7253.
Carr, M. E., Shen, L. L., & Hermans, J. (1977) *Biopolymers 16*, 1−15.
David, A. (1973) *J. Mol. Biol. 76*, 135−148.
Doms, R. W., Keller, D. S., Helenius, A., & Balch, W. E. (1987) *J. Cell Biol. 105*, 1957−1969.
Gaudin, Y., Barge, A., Ebel, C., & Ruigrok, R. W. H. (1995) *Virology 206*, 28−37.
Hantgan, R. R., Braaten, J. V., & Rocco, M. (1993) *Biochemistry 32*, 3935−3941.
Heggeness, M. H., Scheid, A., & Choppin, P. W. (1980) *Proc. Natl. Acad. Sci. U.S.A. 77*, 2631−2635.
Heggeness, M. H., Smith, P. R., & Choppin, P. W. (1982a) *Proc. Natl. Acad. Sci. U.S.A. 79*, 6232−6236.
Heggeness, M. H., Smith, P. R., Ulmanen, I., Krug, R. M., & Choppin, P. W. (1982b) *Virology 118*, 466−470.
Kaptur, P. E., Rhodes, R. B., & Lyles, D. S. (1991) *J. Virol. 65*, 1057−1065.
Knipe, D. M., Baltimore, D., & Lodish, H. (1977) *J. Virol. 21*, 1128−1139.
Koppel, D. E. (1972) *J. Chem. Phys. 57*, 4814−4820.
Lyles, D. S., Varela, V. A., & Parce, J. W. (1990) *Biochemistry 29*, 2442−2449.
Marshall, A. G. (1978) *Biophysical Chemistry: Principles, Techniques, and Applications*, pp 463−480, John Wiley and Sons, New York.
McCreedy, B. J., McKinnon, K. P., & Lyles, D. S. (1990) *J. Virol. 64*, 902−906.
Newcomb, W. W., & Brown, J. C. (1981) *J. Virol. 39*, 295−299.
Newcomb, W. W., Tobin, G. J., McGowan, J. J., & Brown, J. C. (1982) *J. Virol. 41*, 1055−1062.
Odenwald, W. F., Arnheiter, H., Dubois-Dalq, M., & Lazzarini, R. A. (1986) *J. Virol. 57*, 922−932.
Palmer, G. R., & Fritz, O. G. (1979) *Biopolymers 18*, 1659−1672.
Pike, E. R., Pomeroy, W. R. M., & Vaughan, J. M. (1975) *J. Chem. Phys. 62I*, 3188−3192.
Rivas, G. A., Aznarez, J. A., Usobiaga, P., Salz, J. L., & González-Rodríguez, J. (1991) *Eur. Biophys. J. 19*, 335−345.
Thomas, D., Newcomb, W. W., Brown, J. C., Wall, J. S., Hainfeld, J. F., Trus, B. L., & Steven, A. C. (1985) *J. Virol. 54*, 598−607.

BI952001N